Original Article

MOLECULAR METABOLISM

Skeletal glucocorticoid signalling determines leptin resistance and obesity in aging mice

Holger Henneicke [1,2,3,4,10], Sarah Kim [1,5,10], Michael M. Swarbrick [1,5], Jingbao Li [1,6], Sylvia J. Gasparini [1], Joanne Thai [1], Daphne Foong [1], Lauryn L. Cavanagh [1], Colette Fong-Yee [1], Elisabeth Karsten [7], Ruby C.Y. Lin [8,9], Mark S. Cooper [5], Hong Zhou [1,5,*], Markus J. Seibel [1,5]

ABSTRACT

Objective: Aging and chronic glucocorticoid excess share a number of critical features, including the development of central obesity, insulin resistance and osteoporosis. Previous studies have shown that skeletal glucocorticoid signalling increases with aging and that osteoblasts mediate the detrimental skeletal and metabolic effects of chronic glucocorticoid excess. Here, we investigated whether endogenous glucocorticoid action in the skeleton contributes to metabolic dysfunction during normal aging.

Methods: Mice lacking glucocorticoid signalling in osteoblasts and osteocytes ($HSD2^{OB/OCY}$-tg mice) and their wild-type littermates were studied until 3, 6, 12 and 18 months of age. Body composition, adipose tissue morphology, skeletal gene expression and glucose/insulin tolerance were assessed at each timepoint. Leptin sensitivity was assessed by arcuate nucleus STAT3 phosphorylation and inhibition of feeding following leptin administration. Tissue-specific glucose uptake and adipose tissue oxygen consumption rate were also measured.

Results: As they aged, wild-type mice became obese and insulin-resistant. In contrast, $HSD2^{OB/OCY}$-tg mice remained lean and insulin-sensitive during aging. Obesity in wild-type mice was due to leptin resistance, evidenced by an impaired ability of exogenous leptin to suppress food intake and phosphorylate hypothalamic STAT3, from 6 months of age onwards. In contrast, $HSD2^{OB/OCY}$-tg mice remained leptin-sensitive throughout the study. Compared to $HSD2^{OB/OCY}$-tg mice, leptin-resistant wild-type mice displayed attenuated sympathetic outflow, with reduced tyrosine hydroxylase expression in both the hypothalamus and thermogenic adipose tissues. Adipose tissue oxygen consumption rate declined progressively in aging wild-type mice but was maintained in $HSD2^{OB/OCY}$-tg mice. At 18 months of age, adipose tissue glucose uptake was increased 3.7-fold in $HSD2^{OB/OCY}$-tg mice, compared to wild-type mice.

Conclusions: Skeletal glucocorticoid signalling is critical for the development of leptin resistance, obesity and insulin resistance during aging. These findings underscore the skeleton's importance in the regulation of body weight and implicate osteoblastic/osteocytic glucocorticoid signalling in the aetiology of aging-related obesity and metabolic disease.

Keywords Glucocorticoid; Aging; Osteoblast; Osteocyte; Obesity; Leptin; Appetite

[1]Bone Research Program, ANZAC Research Institute, The University of Sydney, Australia [2]Center for Regenerative Therapies TU Dresden, Technische Universität Dresden, Germany [3]Department of Medicine III, Technische Universität Dresden, Germany [4]Center for Healthy Aging, Technische Universität Dresden, Germany [5]Concord Clinical School, The University of Sydney, Australia [6]Key Laboratory for Space Bioscience & Biotechnology, Institute of Special Environmental Biophysics, School of Life Sciences, Northwestern Polytechnical University, China [7]Kolling Institute of Medical Research, The University of Sydney, Australia [8]Centre for Infectious Diseases and Microbiology, Westmead Institute for Medical Research, The University of Sydney, Australia [9]School of Medical Sciences, University of New South Wales Sydney, Australia

[10] Joint first authors.

*Corresponding author. Bone Research Program, ANZAC Research Institute, The University of Sydney, Hospital Road, Concord, NSW 2139, Australia. Fax: +61 2 9767 9101.

E-mails: holger.henneicke@tu-dresden.de (H. Henneicke), sarah.kim1@sydney.edu.au (S. Kim), michael.swarbrick@sydney.edu.au (M.M. Swarbrick), lijingbao@nwpu.edu.cn (J. Li), sylvia.gasparini@tu-dresden.de (S.J. Gasparini), joanne.thai@sydney.edu.au (J. Thai), daphne.foong@sydney.edu.au (D. Foong), lauryn.cavanagh@sydney.edu.au (L.L. Cavanagh), colette.fong-yee@sydney.edu.au (C. Fong-Yee), elisabeth@sanguibio.com (E. Karsten), ruby.lin@sydney.edu.au (R.C.Y. Lin), mark.cooper@sydney.edu.au (M.S. Cooper), h.zhou@sydney.edu.au (H. Zhou), markus.seibel@sydney.edu.au (M.J. Seibel).

Abbreviations: 11β-HSD, 11β-hydroxy-steroid dehydrogenase; ARC, arcuate nucleus; BAT, brown adipose tissue; GTT, glucose tolerance test; IGF-1, insulin-like growth factor 1; ITT, insulin tolerance test; OCR, oxygen consumption rate; PVN, paraventricular nucleus; STAT3, signal transducer and activator of transcription 3; TH, tyrosine hydroxylase; UCP1, uncoupling protein-1

Received August 4, 2020 • Revision received September 28, 2020 • Accepted October 6, 2020 • Available online 10 October 2020

https://doi.org/10.1016/j.molmet.2020.101098

1. INTRODUCTION

Aging is a critical factor for the development of many chronic conditions, including obesity, diabetes, cardiovascular disease and osteoporosis [1]. Older adults have a higher prevalence of metabolic syndrome [2], a phenotypic cluster of central obesity, glucose intolerance, hypertension and dyslipidaemia that markedly increases the risk of cardiovascular disease and diabetes [3]. Adults over 60 years of age are currently the fastest-growing segment of the world's population [4], posing an increasing burden for global public health.

In humans and rodents, aging is characterised by progressive dysfunction of glucocorticoids [5]. Glucocorticoids are pleiotropic hormones required for stress responses, normal development and circadian rhythm; during times of stress, they increase glucose availability and suppress immune function [6]. While circulating glucocorticoid concentrations are regulated by the hypothalamic-pituitary-adrenal axis, their intracellular availability is determined by two enzymes, 11β-hydroxy-steroid dehydrogenase type 1 (11β-HSD1) and type 2 (11β-HSD2). 11β-HSD1 catalyses the formation of active cortisol (in humans) and corticosterone (in rodents) from inactive cortisone and 11-dehydrocorticosterone, respectively [7]. In contrast, 11β-HSD2 converts active glucocorticoids to their inactive metabolites. Increased 11β-HSD1 expression, and therefore increased local glucocorticoid action, has been implicated in the development of the metabolic syndrome in rodents and humans [8]. We and other authors have also found that skeletal 11β-HSD1 expression increases with age in humans [9] and rodents [10,11].

Leptin is an adipocyte-derived hormone produced in proportion to energy stores that regulates the neuroendocrine and metabolic responses to fasting [12]. Leptin inhibits food intake, and concomitantly increases sympathetic outflow to many tissues, including thermogenic brown adipose tissue (BAT) [13]. In obesity, however, exogenous leptin treatment is ineffective for weight loss, due to leptin resistance. Leptin resistance occurs during aging in rodents [14], contributing to weight gain in adulthood.

The skeleton is now recognised as a dynamic endocrine organ, contributing to the regulation of energy homeostasis [15]. Osteocalcin, an osteoblast-derived secreted molecule, influences glucose metabolism by increasing insulin and adiponectin secretion from pancreatic β-cells and adipocytes, respectively [16]. In glucocorticoid-treated mice, we have shown previously that insulin resistance, glucose intolerance, dyslipidaemia and adipose tissue expansion are mediated via the skeleton, specifically through glucocorticoid-induced suppression of osteocalcin [17]. Another osteoblast-derived protein, lipocalin-2, is secreted after feeding and inhibits appetite by binding to and activating the hypothalamic melanocortin-4 receptor [18].

Given the skeleton's role in energy balance, the amplification of skeletal glucocorticoid signalling with aging and the role of osteoblasts and osteocytes in mediating the detrimental metabolic effects of chronic excess glucocorticoids, we hypothesised that disruption of glucocorticoid signalling in osteoblasts and osteocytes would protect mice against obesity and metabolic dysfunction during normal aging. Here, we show that mice in which glucocorticoid signalling was abrogated in osteoblasts and osteocytes (referred to hereafter as $HSD2^{OB/OCY}$-tg mice) were protected against leptin resistance, obesity and insulin resistance during aging. Our findings implicate skeletal glucocorticoid signalling as a key contributor to the aetiology of obesity and the decline in metabolic health with aging.

2. METHODS

2.1. Transgenic mice

$HSD2^{OB/OCY}$-tg mice, in which a truncated 2.3-kb fragment of the proximal promoter and most of the first intron of the rat Pro-a1(I) collagen (*Col1a1)* gene was fused with rat *Hsd11b2* cDNA, leading to expression in osteoblasts and osteocytes, were donated by Barbara Kream (University of Connecticut Health Centre, Farmington, Connecticut, U.S.A.). $HSD2^{OB/OCY}$-tg mice were then crossed with outbred CD-1 mice, resulting in a 1:1 distribution of transgenic mice and wild-type littermates. The main advantage of the CD-1 strain used here was that they breed easily, producing large litters (12 pups/litter). These mice have been extensively characterised in previous studies from our laboratory [11,17,19]. Skeletal expression of the 11βHSD2 transgene was established previously by Sher et al. [20] and in our previous publication [11].

2.2. Housing and study approval

Wild-type and $HSD2^{OB/OCY}$-tg mice were housed at the ANZAC Research Institute, under standard laboratory conditions at 24 °C, with a 12:12-h light—dark cycle and *ad libitum* access to standard chow and water. Food intake was measured every 4—6 weeks. Glucose and insulin tolerance tests, as well as measurement of body composition, were performed prior to sacrifice. The study protocol (#2015/015) was approved by the Sydney Local Health District Animal Ethics Committee, and all research was carried out according to guidelines specified by the National Health and Medical Research Council (NHMRC) of Australia.

2.3. Body composition

Lean and fat mass measurements were performed by dual-X-ray absorptiometry, using a Lunar PIXImus Densitometer (GE Medical Systems, Parramatta, NSW, Australia) according to the manufacturer's instructions.

2.4. Insulin and glucose tolerance tests

Insulin and glucose tolerance tests (ITTs, GTTs) were performed following a 6-h fasting period. For ITTs, insulin (Humalog, Eli Lilly, Indianapolis, IN, U.S.A.) was injected intraperitoneally at a dose of 0.75 U/kg of body weight. For oral GTTs, a glucose bolus (2 g/kg body weight) was administered by gavage. Blood glucose concentrations were measured using an Accu-check glucometer (Roche, North Ryde, NSW, Australia). Tissue-specific glucose uptake was assessed in 6-h fasted mice as described previously [21].

2.5. Immunohistochemistry

Tissues were fixed in 4% paraformaldehyde for 48 h at 4 °C, paraffin-embedded, cut into 5-μm sections and mounted on glass slides. For adipose tissue, adipocyte size was determined in three representative fields from each haematoxylin and eosin (H&E)-stained section using ImageJ software (National Institutes of Health, U.S.A.). Beige adipocytes were identified by their characteristically dense and multilocular appearance as well as their expression of UCP1.

Antigen retrieval was performed in either 1 mM of citrate buffer (for UCP1 and TH staining of adipose tissues) or in 1 mM of ethylenediaminetetraacetic acid (EDTA) buffer (for ARC phospho-STAT3 staining) at 95 °C for 60 min. Endogenous peroxidase activity was blocked using 3% H_2O_2 for 20 min. Sections were then incubated

overnight with the following primary antibodies: rabbit anti-mouse UCP1 (catalogue # 10983, 1:500 dilution, Abcam, Cambridge, MA, U.S.A.), rabbit anti-mouse TH (catalogue # AB152, 1:200 dilution, Millipore, Temecula, CA, U.SA.) and rabbit anti-mouse phospho-STAT3 (catalogue #9145, 1:200 dilution, Cell Signalling Technology, Danvers, MA, U.S.A.). Following 3 washes in PBS-Triton, the biotinylated anti-rabbit secondary antibody was applied for 1 h at room temperature (1:200 dilution, Vector Laboratories, Burlingame CA, U.S.A.). Sections were then washed in PBS-Triton and incubated with Avidin-Biotin-Peroxidase (Vector Laboratories) for 30 min. After rinsing in PBS-Triton, visualisation was performed using diaminobenzidine (DAKO, Carpinteria, CA, U.S.A.) for 4 min. Slides were rinsed and counter-stained with Harris haematoxylin for 4 min, dehydrated with xylene and cover-slipped.

For adipose expression of TH, 3 representative images were taken across 2 levels at least 200 μm apart and analysed for TH-positive nerve endings. In the brain, 2 (Phospho-STAT3) or 3 (TH) sections from each mouse were assessed for immunoreactive nuclei within the nucleus of interest, defined according to the mouse brain atlas [22]. Quantification was performed using ImageJ software (National Institutes of Health, Bethesda, MD, U.S.A.), and the image processing package Fiji (https://fiji.sc) was used to determine thresholds for positive cells. Investigators were blinded to genotype.

2.6. Indirect calorimetry

Mice were acclimated to metabolic cages for 48 h before a 72 h measurement period. Energy expenditure was measured using an indirect calorimetry system (Promethion M, Sable Systems, Las Vegas, NV, U.S.A.). O_2 consumption and CO_2 production were measured for each mouse at 5-min intervals. The flow rate was 2,000 mL/min. Energy expenditure was calculated using the Weir equation: Kcal/hr $=$ $60*(0.003941*VO_2+0.001106*VCO_2)$. Data acquisition and instrument control were coordinated by MetaScreen v. 1.6.2, and the raw data were processed using ExpeData v. 1.4.3 (Sable Systems) and R statistical packages (R Foundation, Vienna, Austria).

2.7. Assessment of leptin sensitivity

Following a 12-h fast, 3- and 6-month old female wild-type and $HSD2^{OB/OCY}$-tg mice were intraperitoneally (*i.p.*) injected with either saline or recombinant mouse leptin, at a dose of 5 μg/g bodyweight. Food intake in the 24 h following saline/leptin treatment was determined by manual weighing. Three days after the conclusion of the food intake measurement, the same mice were injected with recombinant mouse leptin 30 min prior to sacrifice to visualise central leptin signalling [23].

2.8. β_3-Adrenoceptor agonist treatment

Three- and 18-month-old female wild-type and $HSD2^{OB/OCY}$-tg mice were acclimated to metabolic cages for 48 h prior to *i.p.* injection of the selective β_3-adrenoceptor agonist CL-316,243 (Sigma-Aldrich, St. Louis, MO, U.S.A.) at a dose of 5 μg/g of lean body mass. Metabolic measurements were collected for 24 h following injection.

2.9. Adipose tissue oxygen consumption

The *ex-vivo* oxygen consumption rate (OCR) of adipose tissue was measured using a Seahorse XF analyser (Seahorse Bioscience, Billerica, MA, U.S.A.) as described previously [24]. At sacrifice, adipose tissue was dissected out and maintained in Dulbecco's modified Eagle's medium (DMEM)-F12 culture media at 37 °C, pH 7.4, before being cut into 5 mg pieces, weighed and transferred to an XF-24 islet capture plate. Three to 4 samples were taken from each fat pad. After recording baseline OCR, adenosine triphosphate (ATP) turnover and proton leak were measured by the sequential application of oligomycin (10 μg/mL final concentration) and carbonyl cyanide p-trifluoromethoxyphenylhydrazone (FCCP, final concentration 20 μM, both from Sigma-Aldrich). Non-mitochondrial OCR was determined after adding rotenone and antimycin (Sigma-Aldrich, final concentration 5 μM). To normalise OCR to DNA content, DNA was extracted from adipose tissue explants using TRIZOL (Invitrogen, Scoresby, VIC, Australia).

2.10. Serum biochemistry

Blood was collected through cardiac puncture. Mouse leptin, tumour necrosis factor-α, interleukin (IL)-6, IL-1α, IL-1β, IL-10 and monocyte chemoattractant protein-1 were measured using the Bio-Plex Pro Mouse Diabetes 8-Plex and Bio-Plex Pro Mouse Cytokine 23-plex immunoassay kits, on a Bio-Plex series 100 instrument (Biorad, Hercules, CA, U.S.A.). Serum insulin (Mercodia, Uppsala, Sweden), lipocalcin-2 (R&D Systems, Minneapolis, MN, U.S.A.), insulin-like growth factor 1 (IGF-1, R&D Systems) and osteocalcin (Takara Bio, Mountain View, CA, U.S.A.) were assessed using commercially-available enzyme-linked immunosorbent assay (ELISA) assays. Serum corticosterone levels were analysed by stable isotope dilution liquid chromatography—tandem mass spectrometry (LC—MS/MS) as described previously [25].

2.11. Micro-computed tomography (micro-CT)

Micro-CT analyses of the tibia and L3-vertebra were performed using a Skyscan 1172 (Bruker MicroCT, Kontich, Belgium) as previously described [19]. In short, the spine was immersed in phosphate-buffered saline (PBS) and inserted in the scanner according to the manufacturer's instructions. Scanning was performed at 100 keV, 167 μA, 1,475 ms without filter. Approximately 1,100 projections were collected per sample at a resolution of 7.6 μm per pixel. Three-dimensional (3D) reconstruction and analysis of the samples was performed using NRecon and CTAn software, respectively (Bruker). The region of interest (ROI) was selected using an automated algorithm. Vertebral trabecular bone parameters were quantified for the entire space between the cranial and caudal growth plates of the 3rd lumbar vertebra.

2.12. mRNA expression and array

At sacrifice, the legs were removed, and the femurs and tibiae were dissected and cleared of associated connective tissue. Next, the epiphyses were removed from each bone, and the bones were loaded into a 0.5 ml Eppendorf tube that had been perforated at the bottom using a 21G needle. This tube was then loaded into another 1.5 ml Eppendorf tube. Bone marrow was removed from the bones by centrifugation, using a benchtop centrifuge (Eppendorf 5415D, Eppendorf South Pacific, Macquarie Park, NSW, Australia) at $10{,}000 \times g$ for 30 s.

RNA was extracted from the tibiae and femurs using TRIZOL (Invitrogen), followed by a column clean-up (Nucleuspin, Macherey-Nagel, Düren, Germany) and DNase-treatment. Total skeletal RNA (100 ng) was labelled and hybridised onto Affymetrix Mouse GeneChip Gene 2.1 ST arrays (Affymetrix, Santa Clara, CA, U.S.A.; n $=$ 3 wild-type and $HSD2^{OB/OCY}$-tg mice at each time point), according to the manufacturer's instructions, at the Ramaciotti Centre for Genomics (University of New South Wales, Kensington, NSW, Australia). Affymetrix data were processed using the standard approach described in the *Affymetrix I GeneChipExpression Analysis Technical Manual* (2006). Robust multiarray averaging (RMA) was used for background

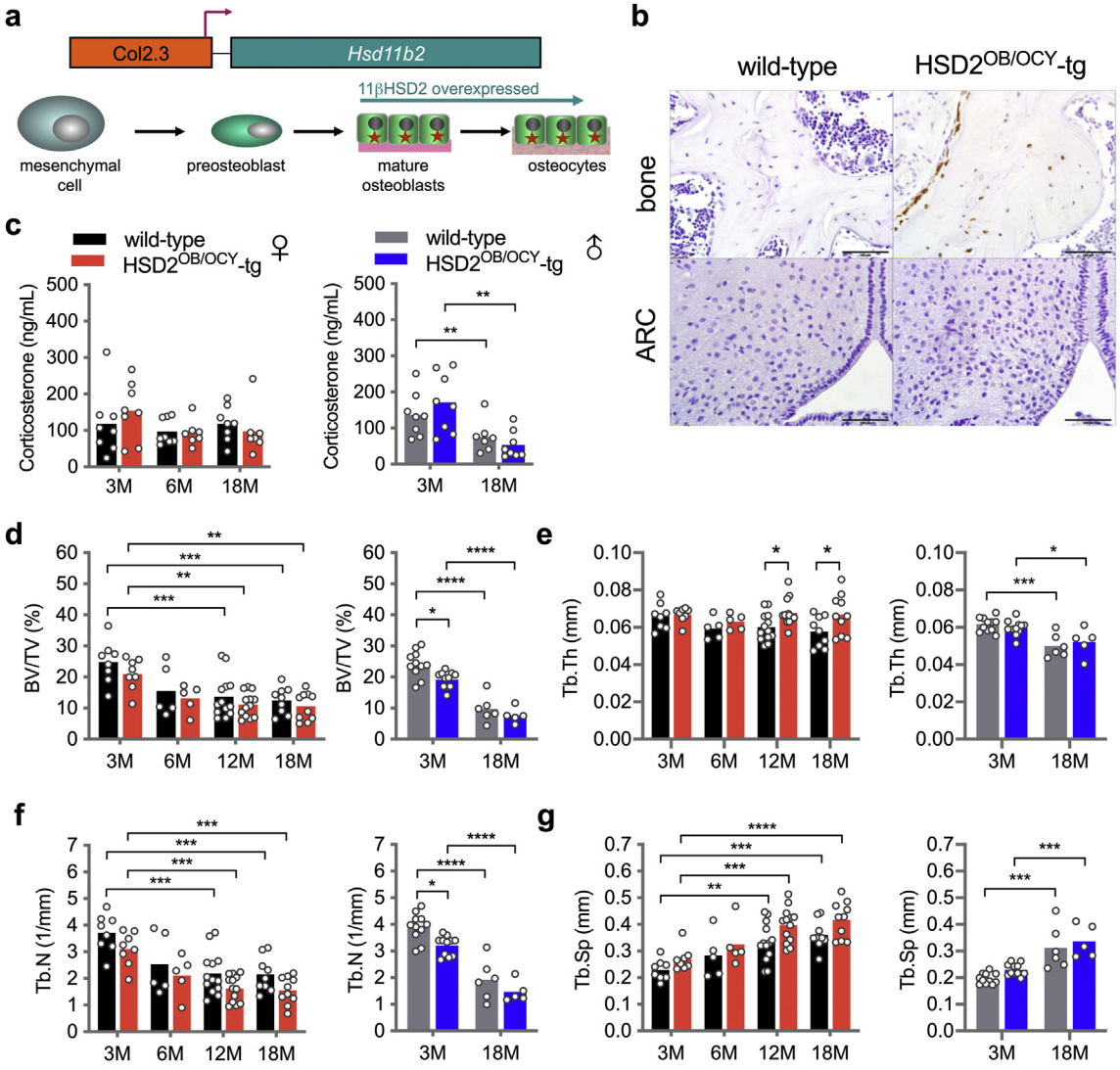

Figure 1: Description and bone phenotype of mice overexpressing *Hsd11b2* in osteoblasts (HSD2$^{OB/OCY}$-tg mice). (a) Here, we used transgenic (HSD2$^{OB/OCY}$-tg) mice expressing *Hsd11b2* cDNA in osteocytes and osteocytes, under the control of a 2.3 kb fragment of the rat Pro-a1(I) collagen (*Col1a1*) proximal promoter and first intron (see Methods). (b) 11β-HSD2 immunohistochemistry of bone and hypothalamus (ARC, arcuate nucleus) from wild-type and HSD2$^{OB/OCY}$-tg mice. (c) Serum corticosterone concentrations in female (left) and male (right) wild-type and HSD2$^{OB/OCY}$-tg mice at 3, 6 and 18 months of age (3 and 18 months only in males). Data are shown as scatterplots, with mean values shown as columns. Differences between wild-type and HSD2$^{OB/OCY}$-tg mice were assessed by two-way ANOVA, with Tukey's *post hoc* tests. *, **, *** and **** indicate $p < 0.05$, $p < 0.01$, $p < 0.001$ and $p < 0.0001$, respectively. (d) Bone volume/total volume (BV/TV, %), (e) trabecular thickness (Tb. Th), (f) trabecular number (Tb. N.) and (g) trabecular separation (Tb. Sp.) from vertebral micro-Ct analysis of female and male wild-type and HSD2$^{OB/OCY}$-tg mice at each timepoint.

correction; this adjusts probe intensities for a number of properties, such as fragment length, GC content, and sequence allele position. RMA normalised data (n = 24) were next subjected to analysis of variance (ANOVA) to examine differential gene expression between genotypes at all age groups (Genomics Suite 6.5, Partek, Inc., St. Louis, MO, U.S.A.). We interrogated the differentially expressed (DE) gene lists in the context of biological processes and systems at unadjusted $p < 0.05$ level (based on Gene Ontology) to avoid exclusion of affected biologically relevant genes that may have been otherwise filtered out. Furthermore, DE genes were visualised in the context of biologically relevant regulatory network using Ingenuity Pathway Analysis (Qiagen, Hilden, Germany, https://www.qiagenbioinformatics.com/products/ingenuity-pathway-analysis/).

2.13. Statistical analysis

Analyses were performed using Prism 8 for macOS software (GraphPad, San Diego, CA, U.S.A.). All continuous variables were first assessed for normality using the Kolmogorov–Smirnov test. Comparisons between wild-type and HSD2$^{OB/OCY}$-tg mice at isolated timepoints were performed using Student's *t*-tests or Mann–Whitney tests, as appropriate. Otherwise, inter-group comparisons across timepoints were assessed by two-way ANOVA, with Tukey's *post hoc*

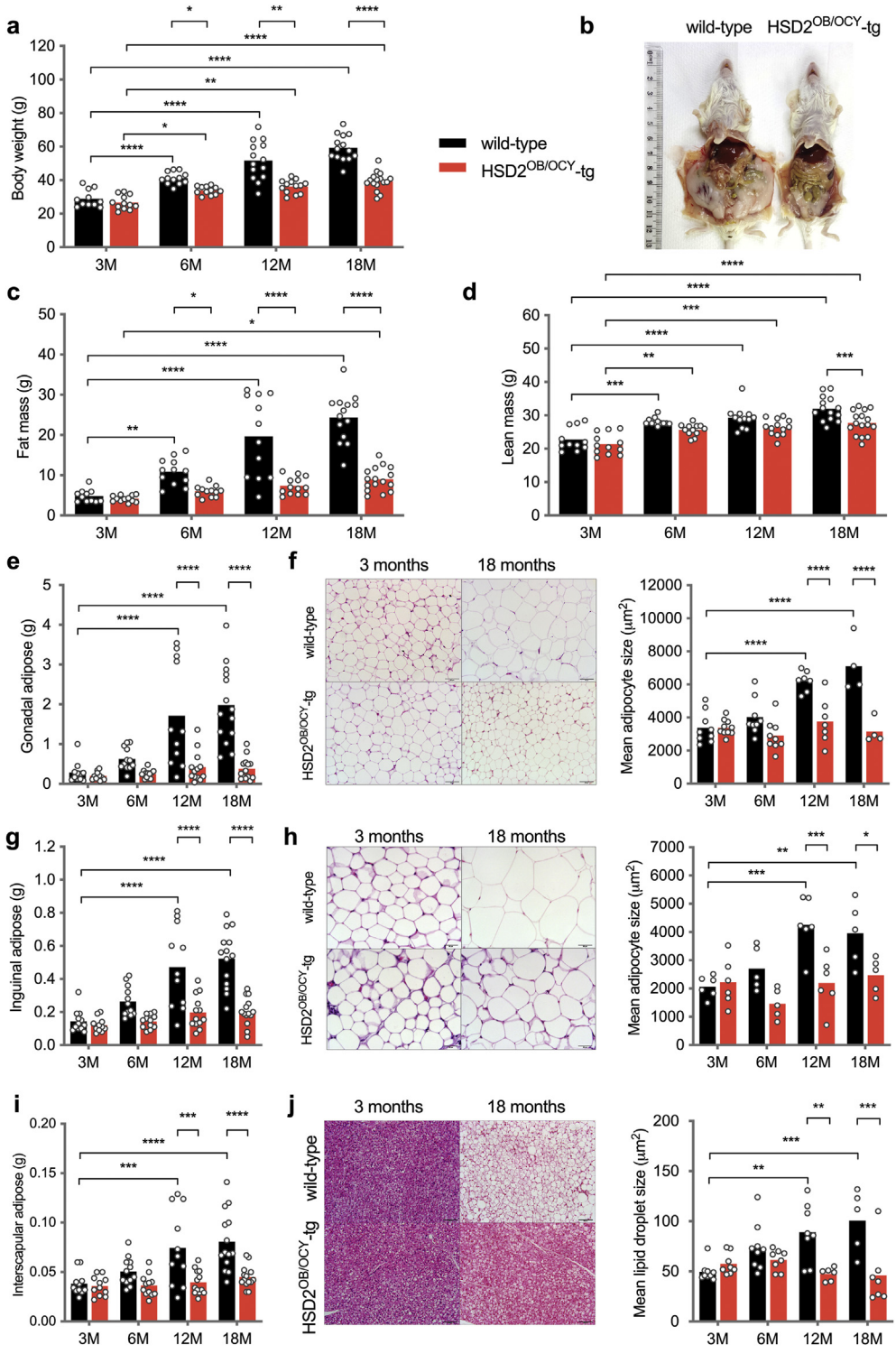

Figure 2: Disruption of glucocorticoid signalling in osteoblasts and osteocytes protects against aging-related obesity in female mice. (a) Body weight, (c) fat mass and (d) lean mass in female wild-type and HSD2$^{OB/OCY}$-tg mice at 3, 6, 12 and 18 months of age. Data are shown as scatterplots, with mean values shown as columns. Differences between wild-type and HSD2$^{OB/OCY}$-tg mice were assessed by two-way ANOVA, with Tukey's *post hoc* tests. *, **, *** and **** indicate $p < 0.05$, $p < 0.01$, $p < 0.001$ and $p < 0.0001$, respectively. Representative photographs of a female littermate pair at 18 months of age are shown in (b). (e) Gonadal adipose weight. (f) Representative images of H&E stained gonadal adipose tissue and measurement of adipocyte size, scale bar = 100 µm. (g) Inguinal adipose weight. (h) Representative images of H&E stained inguinal adipose tissue and measurement of adipocyte size, scale bar = 50 µm. (i) Interscapular BAT weight. (j) Representative images of H&E stained BAT and measurement of lipid droplet size, scale bar = 100 µm. Results for male mice are shown in Figure S2.

tests for pair-wise comparisons. Two-tailed p-values <0.05 were considered significant.

3. RESULTS

3.1. Disruption of glucocorticoid signalling in osteoblasts and osteocytes prevents fat accumulation during normal aging

To investigate the effects of disrupting skeletal glucocorticoid signalling, we studied mice overexpressing the rat *Hsd11b2* mRNA in osteoblasts and osteocytes (HSD2$^{OB/OCY}$-tg mice) under the control of the rat Pro-a1(I) collagen (*Col1a1)* promoter (Figure 1A). As expected, 11β-HSD2 protein was detected in osteoblasts and osteocytes of HSD2$^{OB/OCY}$-tg mice but not in wild-type littermates (Figure 1B). Previous studies utilising this Col2.3 promoter have shown that the transgene is not expressed in lung, bladder, aorta, heart, brain, liver, spleen, thymus, muscle, kidney, intestine or fat of young adult transgenic mice [20,26]. Similarly, we did not detect any *Hsd11b2* mRNA expression in the livers, adipose tissues (inguinal, gonadal), skeletal muscles or hypothalami of HSD2$^{OB/OCY}$-tg mice at 6 months of age (Figure S1). 11β-HSD2 protein was not detected in the hypothalamic arcuate nucleus (ARC) of either wild-type or HSD2$^{OB/OCY}$-tg mice (Figure 1B).

Six cohorts of wild-type and HSD2$^{OB/OCY}$-tg mice were fed chow and studied from 3 to 18 months of age (females were studied at 3, 6, 12 and 18 months, and males were studied at 3 and 18 months). We did not observe any differences in circulating corticosterone concentrations between wild-type and HSD2$^{OB/OCY}$-tg mice, when sampled either during the middle of the day (Figure 1C) or at night (Figure S2a). As in previous studies [19,20], HSD2$^{OB/OCY}$-tg mice of both sexes displayed a mild skeletal phenotype, with slightly lower vertebral bone mass and trabecular number and greater trabecular thickness and separation compared to wild-type mice (Figure 1D–G).

The most striking effect of disrupting skeletal glucocorticoid signalling was that it reduced weight gain, particularly in females (Figs. 2a and S2). In wild-type females, weight gain during aging was mostly due to accrual of fat mass, which increased more than 5-fold between 3 and 18 months of age (Figure 2B,C). In contrast, HSD2$^{OB/OCY}$-tg females remained lean during aging; their fat mass was 45% lower than wild-type mice at 6 months of age ($p < 0.05$), and this difference became even more pronounced at older ages (63% lower at 18 months, $p < 0.0001$).

Lean mass increased with aging in both wild-type and HSD2$^{OB/OCY}$-tg mice (Figure 2D). By 18 months of age, both male and female wild-type mice had gained more lean mass than their HSD2$^{OB/OCY}$-tg littermates (Figures 2D and S2c).

Increased adiposity in wild-type mice was evident in both gonadal (visceral) and inguinal (subcutaneous) fat pad masses (Figure 2E,G). At 18 months of age, gonadal and inguinal fat pads from wild-type mice were 5- and 2-fold greater in mass, respectively, than the equivalent depots in HSD2$^{OB/OCY}$-tg mice. Gonadal and inguinal fat depots did not increase significantly in mass in HSD2$^{OB/OCY}$-tg mice during aging. Increased adiposity in wild-type mice during aging was associated with adipocyte hypertrophy: mean adipocyte size in these depots was doubled in wild-type mice by 12 months of age but remained constant in HSD2$^{OB/OCY}$-tg mice (Figure 2F,H). Similarly, interscapular brown adipose tissue (BAT) increased in mass with aging in wild-type mice; however, this was due to a significant increase in lipid accumulation rather than expansion of healthy BAT (Figure 2I,J). This "whitening" of BAT was not observed in HSD2$^{OB/OCY}$-tg mice: both depot mass and lipid droplet size did not change significantly during aging.

3.2. Disruption of glucocorticoid signalling in osteoblasts and osteocytes prevents insulin resistance with aging, and increases adipose tissue glucose uptake

We also investigated whether the observed differences in adiposity between wild-type and HSD2$^{OB/OCY}$-tg mice were associated with altered glucose metabolism. No significant differences in glucose tolerance between genotypes were observed at 3, 6, 12 or 18 months of age (Figures 3A and S3a). Insulin tolerance was also assessed at each timepoint. Although glycaemic responses to insulin were comparable between female wild-type and HSD2$^{OB/OCY}$-tg mice at 3 months of age (Figure 3B), a difference between genotypes became evident at older ages (Figure 3C, overall effect of genotype: $F_{(1,60)} = 4.93$, $p = 0.030$, two-way ANOVA). Consistent with insulin resistance, female wild-type mice developed fasting hyperinsulinaemia at 12 and 18 months of age (Figure 3D). In males, similarly, insulin resistance and fasting hyperinsulinaemia developed in older wild-type mice, but not HSD2$^{OB/OCY}$-tg mice (Figure S3).

During aging, we observed a small but statistically significant decline in fasting glycaemia in both wild-type and HSD2$^{OB/OCY}$-tg females (Figure 3E). In wild-type mice, this finding suggested that hepatic insulin action (i.e., the suppression of gluconeogenesis) was intact during aging, but that insulin-stimulated glucose uptake in peripheral tissues (adipose, skeletal muscle) was impaired. This led us to measure tissue-specific glucose uptake in 6- and 18-month-old female wild-type and HSD2$^{OB/OCY}$-tg mice using a radio-labelled glucose tolerance test (Figure 3F). At 6 months of age, glucose uptake into peripheral tissues was not different between wild-type and HSD2$^{OB/OCY}$-tg mice. In 18-month-old mice, however, adipose tissue glucose uptake was increased more than five-fold in HSD2$^{OB/OCY}$-tg mice, relative to wild-type mice ($p < 0.0001$). To account for differences in adipose tissue cellularity between wild-type and HSD2$^{OB/OCY}$-tg mice, we normalised adipose tissue glucose uptake to DNA content (Figure S4a). Adipose tissue glucose uptake was increased 3.7-fold in HSD2$^{OB/OCY}$-tg mice compared to wild-type mice ($p = 0.037$). Glucose uptake into interscapular BAT also tended to be greater in HSD2$^{OB/OCY}$-tg than in wild-type mice (1.77-fold increase, $p = 0.074$). No differences in glucose uptake into skeletal muscle or bone were observed at 18 months of age.

3.3. Aging wild-type but not HSD2$^{OB/OCY}$-tg mice develop leptin resistance and hyperphagia

To discern the basis for differences in adiposity between wild-type and HSD2$^{OB/OCY}$-tg mice, we measured energy expenditure and food intake. There were no differences between wild-type and HSD2$^{OB/OCY}$-tg mice for daytime or nighttime energy expenditure, adjusted for lean mass, at any time point examined (Figure 4A). From 5 months of age, however, daily food intake was increased by 18% in wild-type mice, relative to HSD2$^{OB/OCY}$-tg mice, and it remained significantly higher until mice were 12 months old (Figure 4B). This finding suggested that increased food intake in wild-type mice preceded the differences in body weight and adiposity observed at 6 months of age (Figure 2A,B). Therefore, wild-type mice increased their food intake and became obese with aging, while HSD2$^{OB/OCY}$-tg mice in the absence of aging-associated hyperphagia maintained a lean phenotype.

Consistent with the observed increase in fat mass and adipocyte hypertrophy, serum leptin concentrations increased with aging in wild-type but not HSD2$^{OB/OCY}$-tg mice (Figure 4C). At 6 months of age, leptin concentrations were 4-fold higher in wild-type mice, compared to HSD2$^{OB/OCY}$-tg mice ($p < 0.01$), and this difference grew to 6-fold at

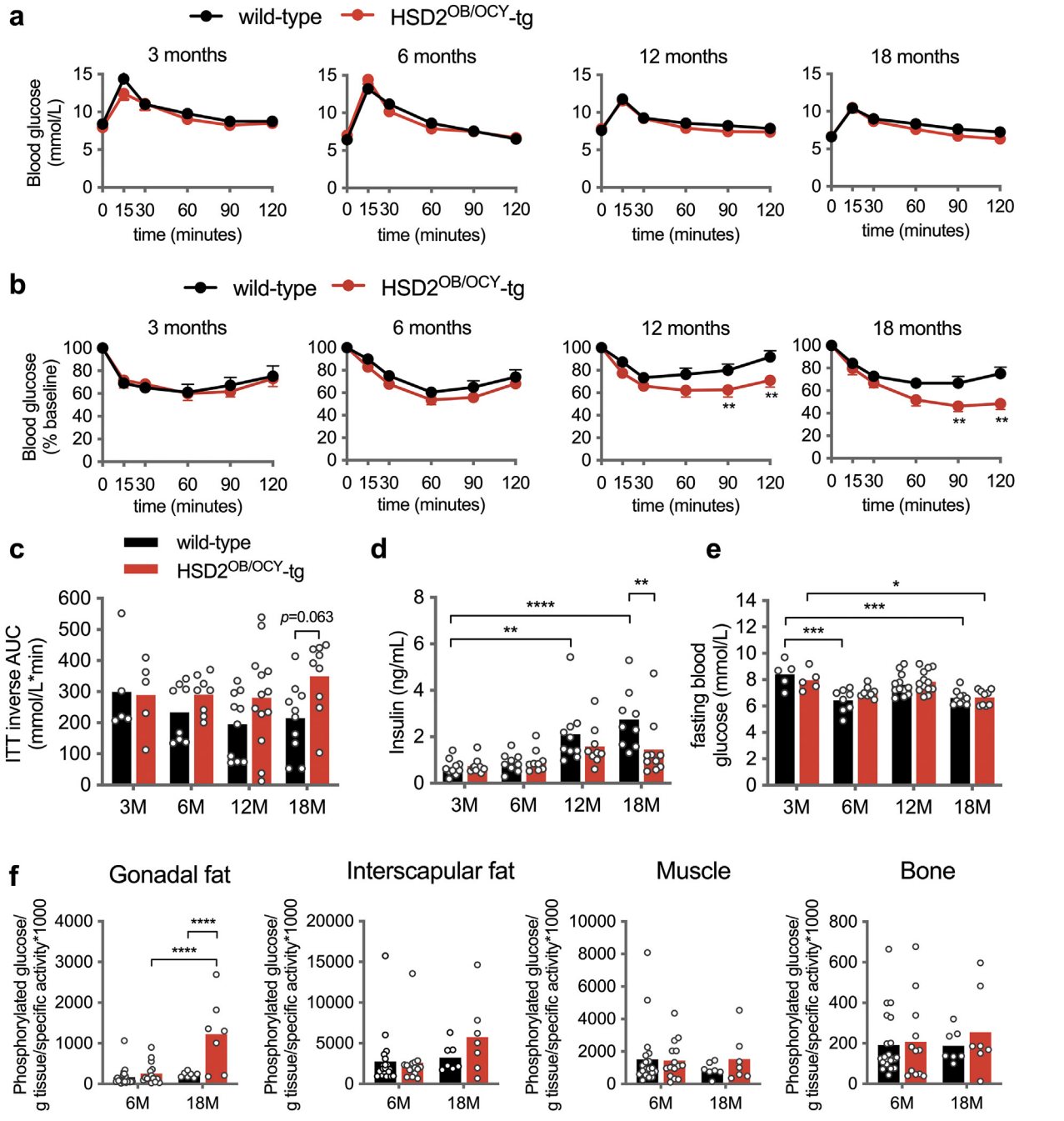

Figure 3: Female HSD2$^{OB/OCY}$-tg mice were protected against insulin resistance associated with aging. (a) Oral glucose tolerance test (oGTT) in female wild-type and HSD2$^{OB/OCY}$-tg mice aged 3, 6, 12 and 18 months ($n = 7-10$/group). Mean ± SEM is shown. (b) Insulin tolerance test (ITT) in female wild-type and HSD2$^{OB/OCY}$-tg mice aged 3, 6, 12 and 18 months ($n = 7-10$/group). Mean ± SEM is shown. (c) ITT inverse area under the curve (AUC). Data are shown as scatterplots, with mean values shown as columns. Differences between wild-type and HSD2$^{OB/OCY}$-tg mice were assessed by two-way ANOVA, with Tukey's *post hoc* tests. *, **, *** and **** indicate $p < 0.05$, $p < 0.01$, $p < 0.001$ and $p < 0.0001$, respectively. The effect of genotype was significant by two-way ANOVA ($F_{(1,60)} = 4.93$, $p = 0.030$). (d) Fasting serum insulin concentrations and (e) fasting blood glucose concentrations. (f) Tissue-specific glucose uptake. Results for male mice are shown in Figure S3.

12 months ($p < 0.001$) and 8-fold at 18 months ($p < 0.0001$ vs. HSD2$^{OB/OCY}$-tg mice). In keeping with the observed changes in food intake, these results suggested that wild-type mice developed leptin resistance during normal aging, while mice with disrupted skeletal glucocorticoid signalling remained leptin sensitive.

In female HSD2$^{OB/OCY}$-tg mice, but not wild-type females, fasting serum IGF-1 concentrations decreased significantly between 3 and 6 months of age (Figure 4D). At 18 months of age, IGF-1 concentrations in HSD2$^{OB/OCY}$-tg mice were 18% lower than in wild-type mice ($p < 0.01$). Similar results were obtained in males (Figure S3e).

Assessment of leptin resistance in mice requires measurement of food intake and central STAT3 phosphorylation following leptin administration [12]. In young, 3-month-old female mice, leptin administered intraperitoneally (5 μg/g bodyweight) significantly suppressed food

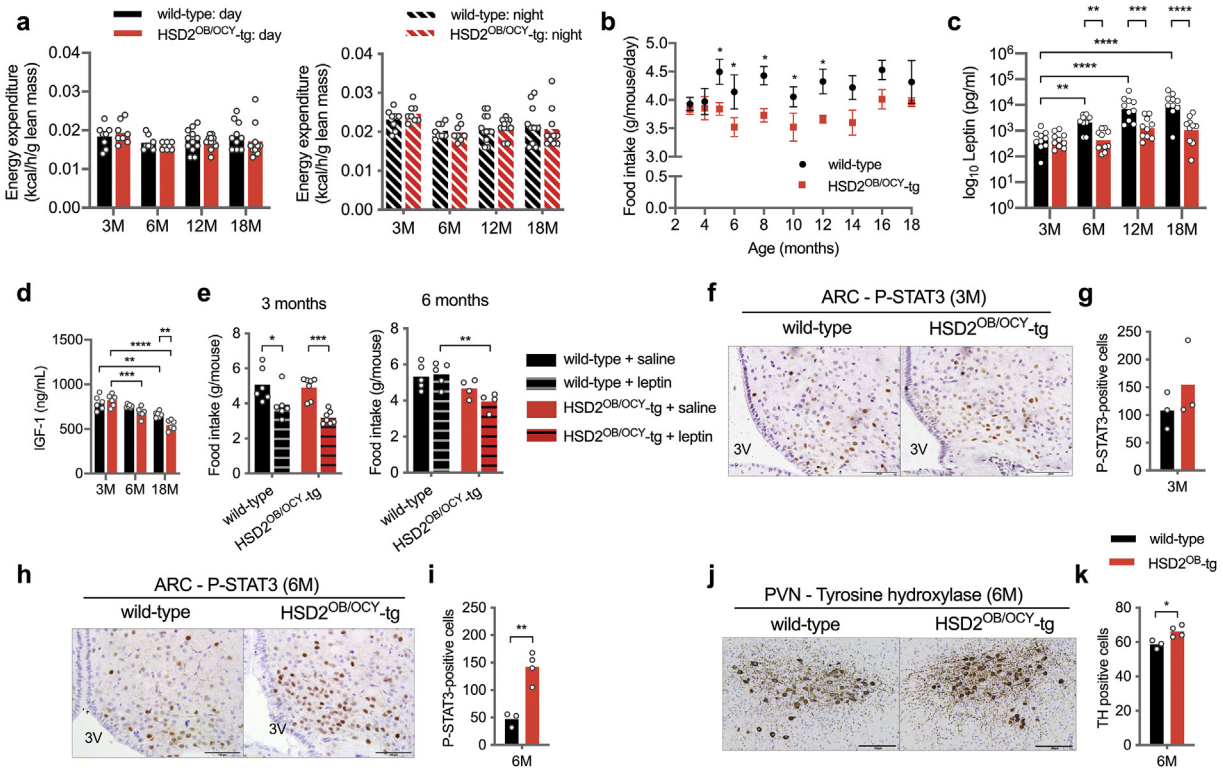

Figure 4: Female HSD2$^{OB/OCY}$-tg mice maintained normal leptin sensitivity with aging. (a) Daytime and nighttime energy expenditure in mice aged 3, 6, 12 and 18 months. Data are shown as scatterplots, with mean values shown as columns. (b) Food intake in wild-type and HSD2$^{OB/OCY}$-tg mice ($n = 3$–12/group, 1$n = 1$ cage, mean ± SEM is shown). (c) Fasting serum leptin (logarithmic scale) and (d) IGF-1 concentrations. (e) Twenty-four-hour food intake after *i.p.* injection of leptin (5 μg/g body weight) at 3 and 6 months of age. (f, g) Representative images of the arcuate nucleus (ARC) stained for phospho-STAT3 (P-STAT3), and quantification in 3-month-old mice. 3V – 3rd ventricle, scale bar = 100 μm. (h, i) Representative images of the ARC stained for P-STAT3 and quantification in 6-month-old mice, scale bar = 100 μm. (j, k) Representative images of the paraventricular nucleus (PVN) stained for tyrosine hydroxylase, and quantification in 6-month-old mice. Scale bar = 200 μm. Comparisons in figures (a)–(e) were made by two-way ANOVA, with Tukey's *post hoc* tests. Comparisons in (g), (i) and (k) were made using Student's *t*-tests. *, **, *** and **** indicate $p < 0.05$, $p < 0.01$, $p < 0.001$ and $p < 0.0001$, respectively.

intake in wild-type and HSD2$^{OB/OCY}$-tg mice (by 22.4 and 34.9%, respectively, Figure 4E). At 6 months of age, however, mean food intake after leptin administration increased by 2.5% in wild-type mice, compared to a 15.4% reduction in HSD2$^{OB/OCY}$-tg mice ($p = 0.0054$). In 6-month-old females, the overall effect of genotype on food intake was highly significant ($F_{1,14} = 13.57$, $p = 0.0025$, two-way ANOVA, Figure 4E).

Next, we assessed central leptin signalling in the hypothalamic arcuate nucleus (ARC) 30 min after a leptin injection. The ARC is a major site of leptin receptor expression, and of defective leptin-induced STAT3 phosphorylation in obesity [23]. At 3 months of age, leptin-activated STAT3 phosphorylation was similar in wild-type and HSD2$^{OB/OCY}$-tg females (Figure 4F,G). At 6 months of age, however, leptin-induced STAT3 phosphorylation was attenuated in wild-type female mice but remained intact in HSD2$^{OB/OCY}$-tg females (Figure 4H,I). Therefore, wild-type mice developed central leptin resistance between 3 and 6 months of age, whereas leptin sensitivity was maintained with age in HSD2$^{OB/OCY}$-tg mice.

In addition to impaired suppression of feeding, mice with defective leptin receptor-associated STAT3 phosphorylation have reduced sympathetic outflow to thermogenic adipose tissues [27]. The paraventricular nucleus (PVN) is a downstream target of ARC leptin signalling and a critical centre for sympathetic regulation. We found that compared to age-matched wild-type females, 6-month old HSD2$^{OB/OCY}$-tg female mice possessed 13% more PVN neurons that were immunoreactive for tyrosine hydroxylase (TH), the rate limiting enzyme for catecholamine synthesis ($p < 0.05$, Figure 4J,K).

3.4. Disruption of skeletal glucocorticoid signalling maintains sympathetic tone and thermogenic beige adipocytes during aging

Because wild-type, but not HSD2$^{OB/OCY}$-tg mice developed leptin resistance from 6 months of age, and given their differences in PVN tyrosine hydroxylase expression, we next investigated sympathetic outflow to thermogenic adipose tissues. In BAT, accordingly, we found that both the number and total area of sympathetic nerve endings declined with age in wild-type mice, while remaining constant in HSD2$^{OB/OCY}$-tg mice (Figure 5A–C).

Distinct from BAT, histological examination of the gonadal fat pads of 3-month-old wild-type and HSD2$^{OB/OCY}$-tg females revealed densely populated areas of uncoupling protein-I (UCP1)-positive multilocular adipocytes (Figure 5D). At 18 months of age, these clusters of 'beige' adipocytes were absent from the gonadal fat of wild-type females but were maintained in HSD2$^{OB/OCY}$-tg mice (Figure 5E,F). Similarly, TH-positive nerve terminals were barely detectable in wild-type mice from 12 months of age, while their numbers were maintained in HSD2$^{OB/OCY}$-tg mice (Figure 5G). Given the increased glucose uptake in

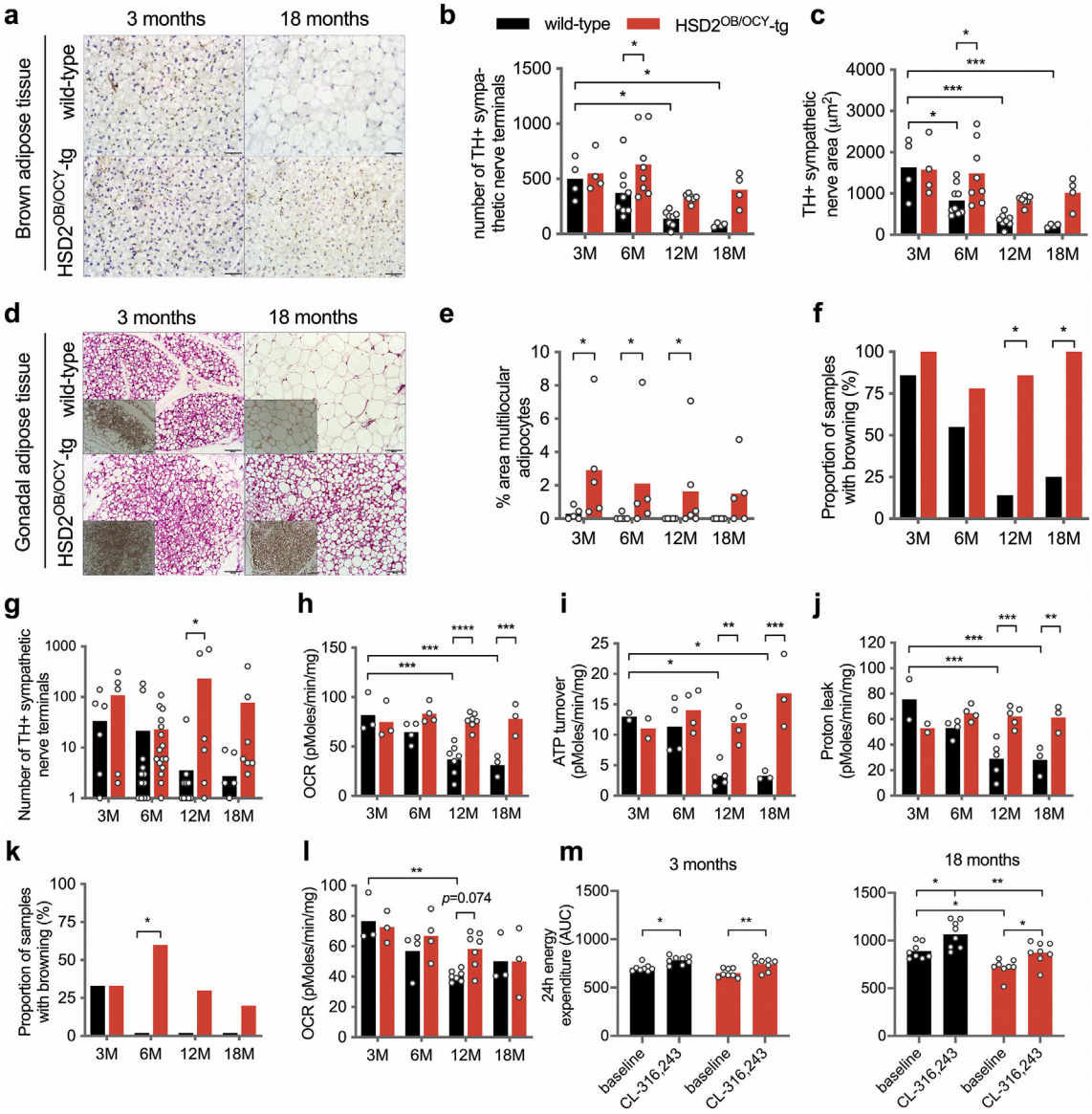

Figure 5: Female HSD2$^{OB/OCY}$-tg mice maintained adipose tissue energy expenditure with aging. (a) Representative images of tyrosine hydroxylase (TH)-stained sections of BAT from young and aged wild-type and HSD2$^{OB/OCY}$-tg mice; scale bar = 50 µm. (b, c) Number of, and area covered by, sympathetic nerve endings in BAT. Data are shown as scatterplots, with mean values shown as columns. (d) Representative images of H&E stained gonadal adipose tissue, showing regions of beige adipocytes, from young and aged wild-type and HSD2$^{OB/OCY}$-tg mice. Insets show UCP1 staining; scale bar = 100 µm. (e) Multilocular adipocyte area in gonadal adipose tissue. (f) Proportion of samples showing presence of beige cells in gonadal adipose tissue (n = 6–8/group). (g) Number of TH-positive nerve terminals in gonadal adipose tissue (logarithmic scale). (h, i, j) Oxygen consumption rate (OCR), ATP turnover and proton leak measured *ex vivo* in gonadal adipose tissue from 3-, 6-, 12- and 18-month-old female wild-type and HSD2$^{OB/OCY}$-tg mice. (k) Proportion of samples showing presence of beige cells in inguinal adipose tissue (n = 6–8/group). (l) Oxygen consumption rate (OCR) measured *ex vivo* in inguinal adipose tissue of 3-, 6-, 12-, and 18-month-old female wild-type and HSD2$^{OB/OCY}$-tg mice. (m) Twenty-four-hour energy expenditure following injection with saline or CL-316,243 (5 µg/g lean body mass) in female wild-type and HSD2$^{OB/OCY}$-tg mice aged 3 and 18 months. Comparisons between groups were performed by two-way ANOVA (except (f) and (k), in which χ^2-tests were used), and Tukey's *post hoc* tests were used for pairwise comparisons. $^*p < 0.05$, $^{**}p < 0.01$, $^{***}p < 0.001$ and $^{****}p < 0.0001$ for comparisons.

gonadal fat from HSD2$^{OB/OCY}$-tg mice (Figure 3F) these results led us to investigate oxygen consumption in adipose tissue.

Ex vivo OCR measurement in gonadal fat explants from female mice aged 3–18 months revealed that total OCR declined significantly with age in wild-type but not in HSD2$^{OB/OCY}$-tg mice (Figure 5H). Similarly, both ATP turnover (UCP1-independent OCR) and proton leak (UCP1-dependent OCR) declined significantly with age in explants from wild-type but not HSD2$^{OB/OCY}$-tg mice (Figure 5I,J). Differences in gonadal fat OCR and ATP turnover between 18-month-old wild-type and HSD2$^{OB/OCY}$-tg mice remained significant when normalised for DNA content, a measure of adipose tissue cellularity (Figs. S4b–d). Inguinal adipose tissue from female wild-type mice displayed similar reductions in browning with age (Figure 5K), although the difference between genotypes was much less pronounced (Figure 5L).

The maximal thermogenic capacity of adipose tissue was tested *in vivo* by administration of the selective β3-adrenoceptor agonist CL-316,243 [28]. Both wild-type and HSD2$^{OB/OCY}$-tg female mice at 3 and 18 months of age responded to CL treatment by significantly increasing whole-body energy expenditure (Figure 5M). At 3 months of age, CL treatment increased mean energy expenditure by 11.4% and

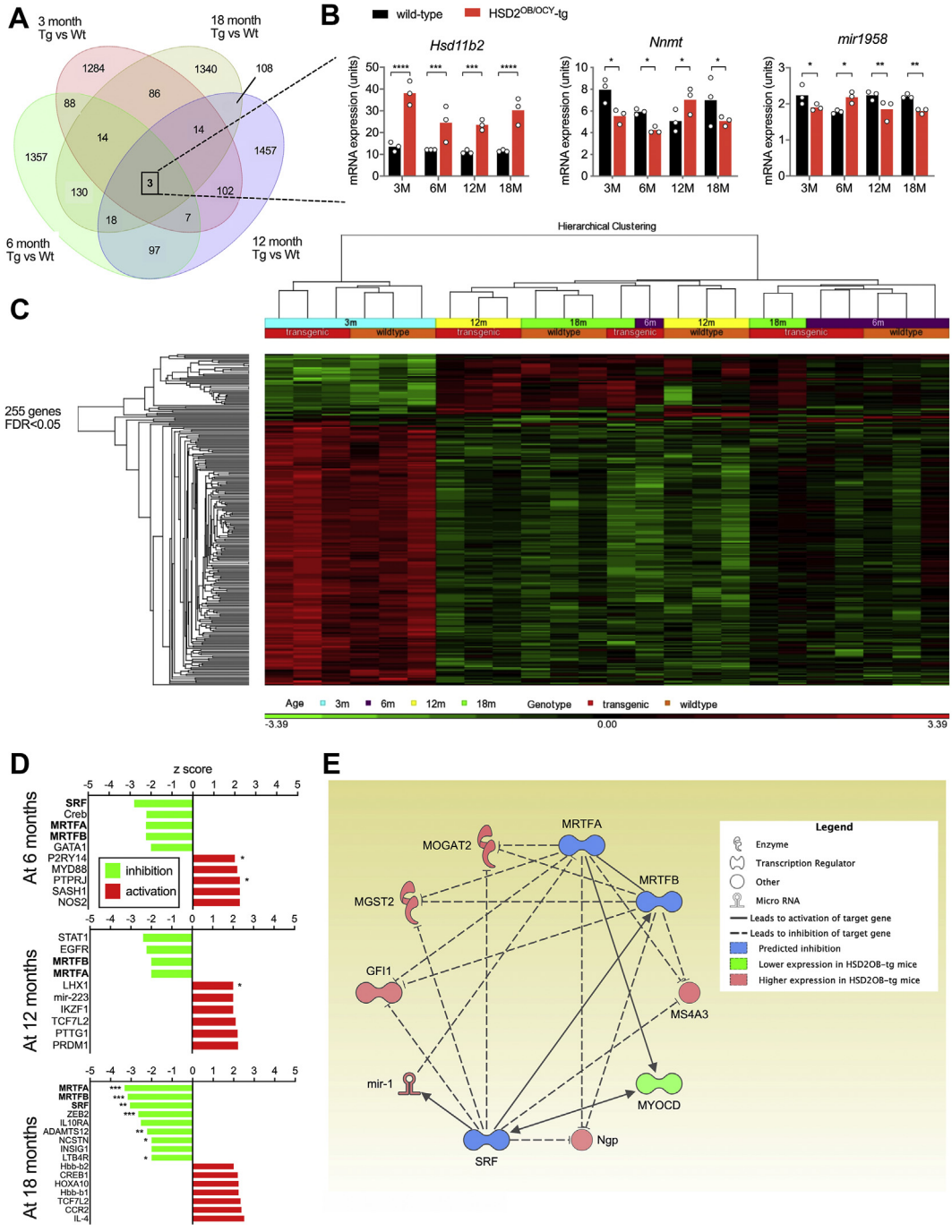

Figure 6: Skeletal gene expression analysis from wild-type and HSD2$^{OB/OCY}$-tg mice during aging, and identification of an SRF-MRTFA-MRTFB gene network in aged HSD2$^{OB/OCY}$-tg mice. (a) Venn diagram of differentially expressed genes in bones from female wild-type and HSD2$^{OB/OCY}$-tg mice, at unadjusted $p < 0.05$, $n = 3$ of each genotype at each timepoint. The number of shared differentially expressed genes at each timepoint (3, 6, 12, 18 months) is shown. (b) Skeletal gene expression levels of *Hsd11b2*, *Nnmt* and *mir-1958* at 3, 6, 12 and 18 months of age. (c) Hierarchical clustering of 255 differentially expressed genes (false discovery rate <0.05) in female wild-type and HSD2$^{OB/OCY}$-tg mice at 3, 6, 12 and 18 months of age. Red indicates upregulated and green indicates downregulated (scale is shown below the chart). (d) Z-scores for upstream regulators of gene expression in the bones of HSD2$^{OB/OCY}$-tg mice, relative to wild-type mice, at 6, 12 and 18 months of age. (e) Putative SRF-MRTFA-MRTFB network at 6–18 months of age in HSD2$^{OB/OCY}$-tg mice. See legend for explanation of symbols. In all cases, $*p < 0.05$, $**p < 0.01$, $***p < 0.001$ and $****p < 0.0001$ for comparisons.

14.2% in wild-type and HSD2$^{OB/OCY}$-tg mice, respectively ($p < 0.05$ for each). Similarly, at 18 months of age, CL treatment significantly increased energy expenditure, by 19.8% in wild-type mice and by 21.6% in HSD2$^{OB/OCY}$-tg mice. Therefore, although adipose tissue OCR declined during aging in wild-type mice, but not HSD2$^{OB/OCY}$-tg mice, the capacity of adipose tissue to produce an appropriate thermogenic response remained intact in both groups. These findings suggested that as they aged, HSD2$^{OB/OCY}$-tg mice were protected against the progressive deterioration in leptin sensitivity and loss of adipose tissue sympathetic outflow seen in wild-type mice.

3.5. HSD2$^{OB/OCY}$-tg mice did not have altered circulating concentrations of osteocalcin or lipocalin-2, compared to wild-type mice

To investigate how disruption of skeletal glucocorticoid signalling could prevent age-related leptin resistance, we measured fasting serum concentrations of osteocalcin and lipocalin-2, two bone-derived peptides reported to influence glucose metabolism and feeding behaviour, respectively [16,18]. Uncarboxylated osteocalcin concentrations declined significantly after 3 months of age in both wild-type and HSD2$^{OB/OCY}$-tg mice but did not differ between the genotypes at any timepoint (Figure S5a). Carboxylated osteocalcin concentrations were, on average, 51% higher in wild-type mice compared to HSD2$^{OB/OCY}$-tg mice ($p < 0.01$) at 3 months of age, but this difference was not maintained during aging (Figure S5b). Fasting lipocalin-2 concentrations increased significantly between 3 and 18 months of age in both wild-type and HSD2$^{OB/OCY}$-tg mice with no significant differences between genotypes at any timepoint (Figure S5c).

3.6. Analysis of skeletal gene expression in bones from wild-type and HSD2$^{OB/OCY}$-tg mice

Gene expression in bone (not including bone marrow) harvested from female wild-type and HSD2$^{OB/OCY}$-tg mice at 3, 6, 12 and 18 months of age was measured by microarray (Figure 6). Across all timepoints, we identified 4,071 differentially expressed genes at $p < 0.05$ (Figure 6A). Three genes were differentially expressed at all 4 timepoints: *Hsd11b2*, nicotinamide N-methyltransferase (*Nnmt*) and *mir1958* (Figure 6B). Of these 3 genes, only *Hsd11b2* displayed a consistent direction of gene expression, being overexpressed 1.86- to 2.79-fold in HSD2$^{OB/OCY}$-tg mice compared to wild-type mice, $0.00082 < p < 4.22 \times 10^{-6}$. *Nnmt* and *mir1958* were not consistently up- or downregulated, and thus did not correlate with the observed phenotype.

Adjustment of these results for a false discovery rate of <0.05 yielded 255 genes. Hierarchical clustering of these genes readily discriminated between wild-type and HSD2$^{OB/OCY}$-tg mice at 3 months of age (Figure 6C) but not at older ages (6—18 months), revealing a pattern of skeletal gene expression comprised of two distinct phases: (i) a high expression level at 3 months of age for most of the differentially-expressed genes, with some differences between wild-type and HSD2$^{OB/OCY}$-tg mice; (ii) a later (6—18 month) phase in which most of the above genes were suppressed, and differences between genotypes were more subtle.

At 3 months of age, bones from HSD2$^{OB/OCY}$-tg mice expressed significantly higher levels of several anti-adipogenic factors, including *A2m*, *Frzb*, *Reck* and *Arhgef24* [29—32] compared to wild-type littermates (Figure S6a). Of note, these genes were only upregulated in HSD2$^{OB/OCY}$-tg mice at 3 months of age and not at older ages.

Next, we analysed the differentially expressed genes at each timepoint using Ingenuity Pathway Analysis. We identified a number of differentially regulated canonical pathways (Supplemental Table 1) and potential upstream regulators (Supplemental Table 2). From 6 months of age onward, we consistently found evidence for suppression of a transcriptional network involving several differentially expressed genes regulated by serum response factor (SRF) and the related myocardin-related transcription factors A and B (MRTFA, MRTFB) in the bones of HSD2$^{OB/OCY}$-tg mice (Figure 6D).

SRF controls genes involved in cell proliferation, differentiation, migration and apoptosis. Its activity is regulated by several cofactors, including the transcription factors MRTFA and MRTFB [33]. White adipose tissue from *Mrtfa*$^{-/-}$ mice contains many more beige adipocytes than equivalent wild-type mice, and they are protected against diet-induced obesity and insulin resistance [34]. Here, suppression of the SRF-MRTFA-MRTFB network in the bones of HSD2$^{OB/OCY}$-tg mice accounted for the observed upregulation/disinhibition of the common target genes *Gfi1*, *Ms4a3*, *Dmkn*, *Mogat2*, *Myocd*, *Ngp* and *Mgst2* (Figs. 6e and S6e).

These findings suggest that the preservation of metabolic health in aging HSD2$^{OB/OCY}$-tg mice involves two distinct phases: firstly, at 3 months of age, an induction of anti-adipogenic factors in the bones of HSD2$^{OB/OCY}$-tg mice; followed by a sustained recruitment of beige adipocytes into white adipose tissue. In HSD2$^{OB/OCY}$-tg mice, therefore, expression of these genes in bone may contribute to the maintenance of normal adiposity, leptin concentrations and leptin sensitivity throughout life.

4. DISCUSSION

Here we investigated the role of skeletal glucocorticoid signalling in the development of aging-related obesity and insulin resistance in mice. In bone, the intracellular availability of active glucocorticoids increases with aging [9—11], and glucocorticoid signalling in osteoblasts and osteocytes is required for the deleterious metabolic effects of chronic glucocorticoid treatment [17]. In the present study, we found that HSD2$^{OB/OCY}$-tg mice were protected against hyperphagia, obesity and insulin resistance, which developed in their wild-type littermates during aging. As they aged, HSD2$^{OB/OCY}$-tg mice remained leptin-sensitive, as demonstrated by their sensitivity to exogenously administered leptin (suppression of appetite and hypothalamic STAT3 phosphorylation), while wild-type mice became leptin-resistant. Differences in leptinaemia and leptin sensitivity between wild-type and HSD2$^{OB/OCY}$-tg mice were evident at 6 months of age, preceding the development of central obesity and peripheral insulin resistance in wild-type mice. The decline in leptin sensitivity in wild-type mice during aging was paralleled by a progressive deterioration in thermogenic adipose tissue function. Therefore, glucocorticoid signalling in osteoblasts and osteocytes is involved in the regulation of appetite, sympathetic tone and adiposity during normal aging.

This study provided us with several important insights. First, we established a new link between local glucocorticoid signalling in osteoblasts and osteocytes and the development of obesity and insulin resistance during aging. Prior studies in mice have indicated that both osteoblasts [35] and osteocytes [36] contribute to the regulation of energy homeostasis and glucose metabolism, but the molecular mechanisms have not been identified. The present study clarifies this issue by showing that local glucocorticoid signalling in these cells is required for aging-related metabolic dysfunction. These findings therefore highlight glucocorticoid signalling in osteoblasts/osteocytes as a new therapeutic target for the treatment and prevention of metabolic disease.

Second, we identified central leptin resistance as the mechanism linking skeletal glucocorticoid signalling with increased food intake and obesity during aging. Wild-type mice developed hyperleptinaemia and leptin resistance at 6 months of age, while HSD2$^{OB/OCY}$-tg mice were leptin-sensitive, remaining normoleptinaemic and lean until 18 months of age. Hyperleptinaemia is required for the development of leptin resistance in mice [37]; we could not confirm this relationship as both were established in wild-type mice at 6 months of age. Regardless, this age of onset corresponded well with other rodent models of leptin resistance [38] and implicated central leptin resistance as an important early factor in the development of obesity, and later, insulin resistance,

during aging. Like other models of improved leptin sensitivity [39,40], serum IGF-1 levels were also lower in HSD2$^{OB/OCY}$-tg mice compared to wild-type mice.

In wild-type mice, central leptin resistance initiated a vicious cycle that contributed to further weight gain. Leptin resistance not only describes a failure of exogenous leptin to suppress appetite, but it is also characterised by reduced sympathetic outflow to thermogenic adipose tissues [13,27]. As they aged, wild-type mice displayed a loss of tyrosine hydroxylase expression in the hypothalamic paraventricular nucleus, as well as a progressive reduction in the density of TH+ sympathetic terminals in white and brown adipose tissues. In HSD2$^{OB/OCY}$-tg mice, however, the density of TH+ nerve terminals in adipose tissues remained constant during aging.

The white adipose tissue oxygen consumption rate declined with aging in wild-type mice, and most of this loss was in UCP1-dependent activity. This progressive loss of adipose tissue thermogenic activity during aging was not due to an inability to respond to thermogenic stimuli, such as β3-AR agonist treatment; it was attributable to reduced sympathetic outflow. However, in HSD2$^{OB/OCY}$-tg mice, adipose tissue OCR was maintained during aging, and glucose uptake into fat was markedly increased. This difference may, in turn, have contributed to the improved peripheral insulin sensitivity in HSD2$^{OB/OCY}$-tg mice during aging.

Third, we found that the effects of disrupting skeletal glucocorticoid signalling on obesity were greater in females than males. Sexual dimorphism for leptin resistance has not been previously described, but differences in circulating leptin concentrations between the sexes are well established in both rodents and humans [41], in part due to differences in fat distribution [42] and the suppressive effects of testosterone [43]. The sexual dimorphism described here may also be due to potentiation of the sympatho-excitatory responses to leptin by oestrogen [44].

We were unable to identify changes in secreted factors from osteoblasts and/or osteocytes that explained the phenotype of HSD2$^{OB/OCY}$-tg mice. Mice deficient in osteocalcin, an osteoblast-derived secreted molecule, have increased adiposity and glycaemia compared to wild-type mice [16], although this finding has been recently challenged [45,46]. We observed differences in carboxylated osteocalcin concentrations between wild-type and HSD2$^{OB/OCY}$-tg mice, but only at 3 months of age; this is consistent with previous reports of impaired mineralisation in HSD2$^{OB/OCY}$-tg mice [20]. Concentrations of both uncarboxylated and carboxylated osteocalcin declined significantly with aging, consistent with skeletal maturation, but had no obvious relationship to the metabolic phenotype of HSD2$^{OB/OCY}$-tg mice.

Another bone-derived factor, lipocalin-2, has been reported to suppress food intake in mice [18]. In HSD2$^{OB/OCY}$-tg mice, fasting serum lipocalin-2 concentrations increased significantly during aging, but no significant differences were observed between wild-type and HSD2$^{OB/OCY}$-tg mice at any timepoint, despite the robust and sustained differences in food intake. We also did not find any difference in skeletal *Lcn* mRNA expression between wild-type and HSD2$^{OB/OCY}$-tg mice. One potential limitation of these results is that we did not measure circulating lipocalin-2 concentrations in our mice at 2–4 h after an extended (16-hour) fast, as described in the original publication [18]. However, the available evidence does not suggest that differences in lipocalin-2 concentrations contribute to the improved leptin sensitivity and protection from obesity in HSD2$^{OB/OCY}$-tg mice.

Other studies of genetically modified mice bred to investigate the contribution of osteoblasts and osteocytes to energy homeostasis have reached similar conclusions. Osteocalcin influences glucose metabolism by stimulating insulin secretion, but it does not regulate appetite or energy expenditure directly [35]. Although osteocalcin-deficient mice were initially reported to have increased visceral adiposity compared to wild-type mice [16], recent studies have not found any effect of deleting osteocalcin on regional adiposity [45] or body weight [45,46]. The contribution of osteocalcin to energy homeostasis is therefore unclear at present. Similarly, studies of lipocalin-2-deficient mice have also reported no perturbation of appetite [47].

Regarding appetite regulation in the current model, two possibilities remain. Firstly, the anorectic effects of inhibiting glucocorticoid signalling in osteoblasts and osteocytes may involve bone-derived hormones other than osteocalcin and lipocalin-2. Studies of mice lacking the prohormone convertase furin in osteoblasts reached a similar conclusion [48]. Alternatively, osteoblasts and osteocytes could regulate food intake and body weight through non-humoral mechanisms. This conclusion is supported by parabiosis experiments between wild-type and lean osteocyte-deficient mice, which showed no effect of the procedure on body weight [36]. Potential non-humoral mechanisms linking bone with the central nervous system include signals indicating integrity of the osteocyte network, which may involve afferent neural circuits from bone [49].

In the present study, circulating corticosterone concentrations decreased significantly with aging in male mice and remained stable in females until 18 months of age. A previous study of male C57BL/6 mice [10] reported higher serum corticosterone levels in male mice at 31 months of age, compared to 4 months of age. We have not measured corticosterone levels in similarly aged mice. Regardless, multiple studies support an increase in skeletal 11β-HSD1 expression, and therefore the intracellular availability of active glucocorticoids, during aging [9–11].

Similar results to ours were described in a recent study of female mice lacking the glucocorticoid receptor (*Nr3c1*) in osteoprogenitor cells [50]. In this study, conditional deletion of *Nr3c1* in *Osx*-Cre-expressing cells led to a 10% reduction in body weight and a mild reduction in bone mass. Circulating corticosterone levels were not affected. Knockout mice also exhibited a marked increase in bone marrow fat content, leading the authors to suggest that glucocorticoid signalling in osteoblastic cells is necessary for bone formation, possibly at the expense of marrow adipogenesis. Notably, *Osx*-Cre is also expressed in stromal cells, adipocytes and perivascular bone marrow cells [51]. We did not assess bone marrow fat in the present study, but we found that at 3 months of age, bones from HSD2$^{OB/OCY}$-tg mice expressed higher amounts of several anti-adipogenic factors (Figure S6a). Further studies will be required to investigate the contribution of glucocorticoid signalling to bone marrow adipogenesis.

Our analysis of gene expression in the bones of wild-type and HSD2$^{OB/OCY}$-tg mice revealed a previously unknown biphasic pattern of gene expression, and highlighted pathways for future investigation. Pathway analysis suggested activation of pro-inflammatory (TLR4) signalling in the bones of HSD2$^{OB/OCY}$-tg mice at 3 months of age (Figure S6c), but we did not find any differences in serum concentrations of several pro-inflammatory cytokines at any timepoint (Figure S5). This suggested that any pro-inflammatory effects were local and transient.

At later timepoints, we found evidence for a sustained suppression of a genetic network involving the related transcription factors SRF, MRTFA and MRTFB (Figure 6), leading to disinhibition of common target genes in HSD2$^{OB/OCY}$-tg mice (Figure S6e). SRF transduces mechanical signals from cytoplasmic actin and is therefore involved in diverse cellular processes, such as proliferation, differentiation, migration and apoptosis. MRTFA and MRTFB are cofactors for SRF and regulate its activity [33]. Similar to the HSD2$^{OB/OCY}$-tg mice studied here, mice lacking MRTFA (*Mrtfa−/−*) not only have reduced bone mass [33] but

also have smaller gonadal, inguinal and interscapular brown fat depots than wild-type mice, lower plasma leptin concentrations and an increased recruitment of beige adipocytes in white adipose tissue [34]. The potential relationships between glucocorticoids, adipogenesis and SRF-MRTFA-MRTFB target genes remain to be investigated in future studies.

5. CONCLUSIONS

This study demonstrates for the first time that glucocorticoid signalling in cells of the osteoblastic lineage has a critical role in the development of leptin resistance and metabolic dysfunction during aging. Our findings not only underscore the importance of the skeleton for the regulation of body weight and whole-body metabolism, but also implicate glucocorticoid signalling in osteoblasts and osteocytes as a novel therapeutic target to alleviate the growing worldwide burden of obesity-related disease.

AUTHOR CONTRIBUTIONS

Conceptualisation: HH, SK, MJS, HZ; formal analysis: HH, SK, MMS; investigation: HH, SK, JL, SJG, JT, DF, LLC, RCYL; resources: CF-Y, EK; writing - original draft: HH, SK, MMS, MJS, HZ; writing - reviewing and editing: HH, SK, MMS, MJS, HZ; visualisation: HH, SK, MMS, HZ; supervision and project administration: MJS, HZ; funding acquisition: MJS, MSC, MMS, HZ.

DATA AVAILABILITY STATEMENT

All data presented in this manuscript are available on request from the authors. Microarray data has been deposited into the Gene Expression Omnibus (accession number GSE141448, https://www.ncbi.nlm.nih.gov/geo/).

ACKNOWLEDGEMENTS

The authors would like to acknowledge the technical assistance of Ling Zhuang and Alma Wu. The authors acknowledge support from the Bosch Institute at the University of Sydney (equipment) and the Ramaciotti Centre for Genomics at the University of New South Wales (microarray). The authors also acknowledge the facilities and the scientific and technical assistance of the Australian Centre for Microscopy and Microanalysis, University of Sydney. We would like to thank the Australian Government for NHMRC project funding (1101879) as well as scholarship support (to HH, SK and SJG).

CONFLICT OF INTEREST

The authors have no conflicts of interest to declare.

APPENDIX A. SUPPLEMENTARY DATA

Supplementary data to this article can be found online at https://doi.org/10.1016/j.molmet.2020.101098.

REFERENCES

[1] Kirkland, J.L., 2013. Translating advances from the basic biology of aging into clinical application. Experimental Gerontology 48(1):1–5.

[2] Aguilar, M., Bhuket, T., Torres, S., Liu, B., Wong, R.J., 2015. Prevalence of the metabolic syndrome in the United States, 2003-2012. JAMA 313(19):1973–1974.

[3] Cornier, M.A., Dabelea, D., Hernandez, T.L., Lindstrom, R.C., Steig, A.J., Stob, N.R., et al., 2008. The metabolic syndrome. Endocrine Reviews 29(7):777–822.

[4] Glatt, S.J., Chayavichitsilp, P., Depp, C., Schork, N.J., Jeste, D.V., 2007. Successful aging: from phenotype to genotype. Biological Psychiatry 62(4):282–293.

[5] Vitale, G., Salvioli, S., Franceschi, C., 2013. Oxidative stress and the ageing endocrine system. Nature Reviews Endocrinology 9(4):228–240.

[6] Sharma, A.K., Shi, X., Isales, C.M., McGee-Lawrence, M.E., 2019. Endogenous glucocorticoid signaling in the regulation of bone and marrow adiposity: lessons from metabolism and cross talk in other tissues. Current Osteoporosis Reports 17(6):438–445.

[7] Tomlinson, J.W., Walker, E.A., Bujalska, I.J., Draper, N., Lavery, G.G., Cooper, M.S., et al., 2004. 11beta-hydroxysteroid dehydrogenase type 1: a tissue-specific regulator of glucocorticoid response. Endocrine Reviews 25(5):831–866.

[8] Cooper, M.S., Stewart, P.M., 2009. 11Beta-hydroxysteroid dehydrogenase type 1 and its role in the hypothalamus-pituitary-adrenal axis, metabolic syndrome, and inflammation. The Journal of Cinical Endocrinology and Metabolism 94(12):4645–4654.

[9] Cooper, M.S., Rabbitt, E.H., Goddard, P.E., Bartlett, W.A., Hewison, M., Stewart, P.M., 2002. Osteoblastic 11beta-hydroxysteroid dehydrogenase type 1 activity increases with age and glucocorticoid exposure. Journal of Bone and Mineral Research 17(6):979–986.

[10] Weinstein, R.S., Wan, C., Liu, Q., Wang, Y., Almeida, M., O'Brien, C.A., et al., 2010. Endogenous glucocorticoids decrease skeletal angiogenesis, vascularity, hydration, and strength in aged mice. Aging Cell 9(2):147–161.

[11] Tu, J., Zhang, P., Ji, Z., Henneicke, H., Li, J., Kim, S., et al., 2019. Disruption of glucocorticoid signalling in osteoblasts attenuates age-related surgically induced osteoarthritis. Osteoarthritis and Cartilage 27(10):1518–1525.

[12] Myers Jr., M.G., Leibel, R.L., Seeley, R.J., Schwartz, M.W., 2010. Obesity and leptin resistance: distinguishing cause from effect. Trends in Endocrinology and Metabolism 21(11):643–651.

[13] Haynes, W.G., Morgan, D.A., Walsh, S.A., Mark, A.L., Sivitz, W.I., 1997. Receptor-mediated regional sympathetic nerve activation by leptin. Journal of Clinical Investigation 100(2):270–278.

[14] Scarpace, P.J., Matheny, M., Shek, E.W., 2000. Impaired leptin signal transduction with age-related obesity. Neuropharmacology 39(10):1872–1879.

[15] Riddle, R.C., Clemens, T.L., 2017. Bone cell bioenergetics and skeletal energy homeostasis. Physiological Reviews 97(2):667–698.

[16] Lee, N.K., Sowa, H., Hinoi, E., Ferron, M., Ahn, J.D., Confavreux, C., et al., 2007. Endocrine regulation of energy metabolism by the skeleton. Cell 130(3):456–469.

[17] Brennan-Speranza, T.C., Henneicke, H., Gasparini, S.J., Blankenstein, K.I., Heinevetter, U., Cogger, V.C., et al., 2012. Osteoblasts mediate the adverse effects of glucocorticoids on fuel metabolism. Journal of Clinical Investigation 122(11):4172–4189.

[18] Mosialou, I., Shikhel, S., Liu, J.M., Maurizi, A., Luo, N., He, Z., et al., 2017. MC4R-dependent suppression of appetite by bone-derived lipocalin 2. Nature 543(7645):385–390.

[19] Kalak, R., Zhou, H., Street, J., Day, R.E., Modzelewski, J.R., Spies, C.M., et al., 2009. Endogenous glucocorticoid signalling in osteoblasts is necessary to maintain normal bone structure in mice. Bone 45(1):61–67.

[20] Sher, L.B., Woitge, H.W., Adams, D.J., Gronowicz, G.A., Krozowski, Z., Harrison, J.R., et al., 2004. Transgenic expression of 11beta-hydroxysteroid dehydrogenase type 2 in osteoblasts reveals an anabolic role for endogenous glucocorticoids in bone. Endocrinology 145(2):922–929.

[21] Hocking, S.L., Stewart, R.L., Brandon, A.E., Suryana, E., Stuart, E., Baldwin, E.M., et al., 2015. Subcutaneous fat transplantation alleviates diet-induced glucose intolerance and inflammation in mice. Diabetologia 58(7):1587–1600.

[22] Franklin, K.B.J., Paxinos, G., 2013. Paxinos and Franklin's the mouse brain in stereotaxic coordinates, ed. Amsterdam: Academic Press, an imprint of Elsevier.
[23] Munzberg, H., Flier, J.S., Bjorbaek, C., 2004. Region-specific leptin resistance within the hypothalamus of diet-induced obese mice. Endocrinology 145(11): 4880–4889.
[24] Dunham-Snary, K.J., Sandel, M.W., Westbrook, D.G., Ballinger, S.W., 2014. A method for assessing mitochondrial bioenergetics in whole white adipose tissues. Redox Biology 2:656–660.
[25] Simanainen, U., Lampinen, A., Henneicke, H., Brennan, T.C., Heinevetter, U., Harwood, D.T., et al., 2011. Long-term corticosterone treatment induced lobe-specific pathology in mouse prostate. The Prostate 71(3):289–297.
[26] Kalajzic, I., Kalajzic, Z., Kaliterna, M., Gronowicz, G., Clark, S.H., Lichtler, A.C., et al., 2002. Use of type I collagen green fluorescent protein transgenes to identify subpopulations of cells at different stages of the osteoblast lineage. Journal of Bone and Mineral Research 17(1):15–25.
[27] Bates, S.H., Dundon, T.A., Seifert, M., Carlson, M., Maratos-Flier, E., Myers Jr., M.G., 2004. LRb-STAT3 signaling is required for the neuroendocrine regulation of energy expenditure by leptin. Diabetes 53(12):3067–3073.
[28] Himms-Hagen, J., Cui, J., Danforth Jr., E., Taatjes, D.J., Lang, S.S., Waters, B.L., et al., 1994. Effect of CL-316,243, a thermogenic beta 3-agonist, on energy balance and brown and white adipose tissues in rats. American Journal of Physiology 266(4 Pt 2):R1371–R1382.
[29] Park, J., Park, J., Nahm, S.S., Choi, I., Kim, J., 2013. Identification of anti-adipogenic proteins in adult bovine serum suppressing 3T3-L1 preadipocyte differentiation. BMB Reports 46(12):582–587.
[30] Higuchi, R.G., Peltz, G.A., Fijal, B., Ro, S.K., Li, J., 2010. In: Office, U.S.P. (Ed.), Associations of polymorphisms in the FRZB gene in obesity and osteoporosis. RocheMolecularSystems,Inc., United States of America.
[31] Mahl, C., Egea, V., Megens, R.T., Pitsch, T., Santovito, D., Weber, C., et al., 2016. RECK (reversion-inducing cysteine-rich protein with Kazal motifs) regulates migration, differentiation and Wnt/beta-catenin signaling in human mesenchymal stem cells. Cellular and Molecular Life Sciences 73(7):1489–1501.
[32] Bryan, B.A., Li, D., Wu, X., Liu, M., 2005. The Rho family of small GTPases: crucial regulators of skeletal myogenesis. Cellular and Molecular Life Sciences 62(14):1547–1555.
[33] Bian, H., Lin, J.Z., Li, C., Farmer, S.R., 2016. Myocardin-related transcription factor A (MRTFA) regulates the fate of bone marrow mesenchymal stem cells and its absence in mice leads to osteopenia. Molecular Metabolism 5(10):970–979.
[34] McDonald, M.E., Li, C., Bian, H., Smith, B.D., Layne, M.D., Farmer, S.R., 2015. Myocardin-related transcription factor A regulates conversion of progenitors to beige adipocytes. Cell 160(1–2):105–118.
[35] Yoshikawa, Y., Kode, A., Xu, L., Mosialou, I., Silva, B.C., Ferron, M., et al., 2011. Genetic evidence points to an osteocalcin-independent influence of osteoblasts on energy metabolism. Journal of Bone and Mineral Research 26(9):2012–2025.
[36] Sato, M., Asada, N., Kawano, Y., Wakahashi, K., Minagawa, K., Kawano, H., et al., 2013. Osteocytes regulate primary lymphoid organs and fat metabolism. Cell Metabolism 18(5):749–758.
[37] Knight, Z.A., Hannan, K.S., Greenberg, M.L., Friedman, J.M., 2010. Hyperleptinemia is required for the development of leptin resistance. PloS One 5(6): e11376.
[38] Morrison, C.D., White, C.L., Wang, Z., Lee, S.Y., Lawrence, D.S., Cefalu, W.T., et al., 2007. Increased hypothalamic protein tyrosine phosphatase 1B contributes to leptin resistance with age. Endocrinology 148(1):433–440.
[39] Briancon, N., McNay, D.E., Maratos-Flier, E., Flier, J.S., 2010. Combined neural inactivation of suppressor of cytokine signaling-3 and protein-tyrosine phosphatase-1B reveals additive, synergistic, and factor-specific roles in the regulation of body energy balance. Diabetes 59(12):3074–3084.
[40] Loh, K., Fukushima, A., Zhang, X., Galic, S., Briggs, D., Enriori, P.J., et al., 2011. Elevated hypothalamic TCPTP in obesity contributes to cellular leptin resistance. Cell Metabolism 14(5):684–699.
[41] Kennedy, A., Gettys, T.W., Watson, P., Wallace, P., Ganaway, E., Pan, Q., et al., 1997. The metabolic significance of leptin in humans: gender-based differences in relationship to adiposity, insulin sensitivity, and energy expenditure. The Journal of Cinical Endocrinology and Metabolism 82(4): 1293–1300.
[42] Van Harmelen, V., Reynisdottir, S., Eriksson, P., Thorne, A., Hoffstedt, J., Lonnqvist, F., et al., 1998. Leptin secretion from subcutaneous and visceral adipose tissue in women. Diabetes 47(6):913–917.
[43] Horlick, M.B., Rosenbaum, M., Nicolson, M., Levine, L.S., Fedun, B., Wang, J., et al., 2000. Effect of puberty on the relationship between circulating leptin and body composition. The Journal of Cinical Endocrinology and Metabolism 85(7):2509–2518.
[44] Brooks, V.L., Shi, Z., Holwerda, S.W., Fadel, P.J., 2015. Obesity-induced increases in sympathetic nerve activity: sex matters. Autonomic Neuroscience 187:18–26.
[45] Moriishi, T., Ozasa, R., Ishimoto, T., Nakano, T., Hasegawa, T., Miyazaki, T., et al., 2020. Osteocalcin is necessary for the alignment of apatite crystallites, but not glucose metabolism, testosterone synthesis, or muscle mass. PLoS Genetics 16(5):e1008586.
[46] Diegel, C.R., Hann, S., Ayturk, U.M., Hu, J.C.W., Lim, K.E., Droscha, C.J., et al., 2020. An osteocalcin-deficient mouse strain without endocrine abnormalities. PLoS Genetics 16(5):e1008361.
[47] Law, I.K., Xu, A., Lam, K.S., Berger, T., Mak, T.W., Vanhoutte, P.M., et al., 2010. Lipocalin-2 deficiency attenuates insulin resistance associated with aging and obesity. Diabetes 59(4):872–882.
[48] Al Rifai, O., Chow, J., Lacombe, J., Julien, C., Faubert, D., Susan-Resiga, D., et al., 2017. Proprotein convertase furin regulates osteocalcin and bone endocrine function. Journal of Clinical Investigation 127(11):4104–4117.
[49] Dimitri, P., Rosen, C., 2017. The central nervous system and bone metabolism: an evolving story. Calcified Tissue International 100(5):476–485.
[50] Pierce, J.L., Ding, K.H., Xu, J., Sharma, A.K., Yu, K., Del Mazo Arbona, N., et al., 2019. The glucocorticoid receptor in osteoprogenitors regulates bone mass and marrow fat. Journal of Endocrinology.
[51] Chen, J., Shi, Y., Regan, J., Karuppaiah, K., Ornitz, D.M., Long, F., 2014. Osx-Cre targets multiple cell types besides osteoblast lineage in postnatal mice. PloS One 9(1):e85161.

